Aza-bridged bisphenanthrolinyl Pt(II) complexes: efficient stabilization and topological selectivity on telomeric G-quadruplexes

Lei He[#1], Zhenyu Meng[#1], Yiqun Xie[#2], Xiang Chen[1], Tianhu Li[1], Fangwei Shao[1]*

[1]*Division of Chemistry and Biological Chemistry, School of Physical and Mathematical Sciences, Nanyang Technological University, Singapore 637371*

[2]*Department of Breast Surgery, Shanghai Huangpu Center Hospital, Shanghai, China 200002*

Abstract

Two platinum complexes with an aza-bridged bis-phenanthroline ligand (bpa) were synthesized. The two phenanthrolines in bpa entered a flat plane prior to binding of nucleic acids, which bestowed on the two Pt complexes a significantly high stabilizing ability on both DNA and RNA G-quadruplexes. Further extending alkyl tail from aromatic coordination core enabled the complexes to distinguish GQ sequence based upon the topological folding structures and enhanced the selectivity of the complex against duplex DNA. This study paved the way to develop Pt complexes as GQ stabilizers for specific folding topology and the applications to disease and/or personalized anticancer medicine/therapy.

Keywords

Pt complex; G-quadruplex; RNA; Telomere; Folding topology; Anti-cancer activity

Introduction

Nucleic acids with guanine rich sequences have a propensity to adopt tetra-stranded intra- and intermolecular quadruplex structures that are stabilized by a stack of planar aromatic guanine quartets (G-tetrad), in which four guanines are held together by noncanonical Hoogsteen hydrogen bonding [1-5]. Formation and stability of the whole G-quadruplex structure usually exhibited monovalent cation-dependent manner: $Li^+<Na^+<K^+$ [6-9]. These G-rich sequences can adopt different topologies with distinct strand orientation, including parallel, antiparallel and parallel/antiparallel hybrids [10-17]. G-quadruplexes (GQ) involved in a number of key cellular processes. The well-known example is the human telomeric DNA, which is consists of tandem arrays of simple G-rich (TTAGGG) repeats over several hundred bases [18-20]. It has been shown that if this single-stranded telomeric DNA folded into a quadruplex, the activity of telomerase will be inhibited and thus impede cell proliferation [21,22]. Recent studies found that telomeric RNA (*TERRA*), which is transcribed from the C-rich strand of telomeric DNA, was involved in chromatin regulation and remodeling, as well as telomerase function [23-25]. Besides, many oncogene promoters possess G-quadruplex folding sequences, such as *c-myc*, *bcl-2* and *c-kit*, form rich GQ topology *in vitro* and *in vivo* [26]. The significant biological roles of G-quadruplex suggested GQ, as a unique family of noncanonical secondary structure, have high potentials as anticancer drug targets for chemotherapeutics.

Up until now, considerable studies focused on the stabilization of G-quadruplexes by using small molecules, such as porphyrin-based complexes and

heteroaromatic organic compounds [27-32]. These compounds with planar aromatic motifs can stack with the multiple layers of G-tetrads at the core of G-quadruplex. At the same time the extensive size and shape of the large aromatic conjugates were also used to distinguish duplex DNA and achieve specific binding to GQs. Besides, sequence and cation dependence of folding polymorphism make it possible to target a specific G-rich sequence by interactions between binding molecules and unique loop arrangements. Consequentially, a GQ stabilizer with binding preference to a specific G-quadruplex topological structure can reach the goal of disease specific and/or personalized medicines.

Metal complexes have been reported to strongly and selectively interact with quadruplex DNA [33-38]. As G-quadruplex binders, metal complexes display several advantageous over their organic counterparts. Metal complex with planar heteroaromatic ligand provided strong π stacking with G-tetrad so that efficiently stabilized G-quadruplexes. Besides, both the coordination geometry of metal center, the ligand size and alkyl tails extended from aromatic moieties were easily tuned to obtain topological recognition of GQ targets. Moreover, the electropositive metal center endowed its interaction with cation cavity at the center of G-quadruplexes. Although these metal complexes have shown excellent binding affinity and stabilization on DNA G-quadruplexes, none of them has been demonstrated as RNA G-quadruplex stabilizer until now.

To date, a lot of platinum complexes have been reported as G-quadruplex stabilizers. The square shape of di-ligand coordination on Pt^{2+} provides the necessary

size and shape of aromatic area for good π-π stacking with G-quartets [39-43]. Metal complexes coordinated with phenanthroline and its derivatives have been widely studied as GQ binders and stabilizers due to its excellent size matched with G-quartet. Herein, we designed and synthesized two platinum complexes with bis(1,10-phenanthrolin-2-yl)amine (bpa) ligand. Two 1,10-phenanthroline (phen) were connected via an aza-bridge and form a planar configuration under acidic condition. Upon coordination, two $[Pt(bpa)]^{2+}$ complexes can enter a rigidly flat geometry and bestow strong π stacking with G quartets to enhance GQ stability. Both Pt complexes exhibited significantly higher stabilization effect towards both DNA and RNA G-quadruplexes than duplex DNA.

Materials and methods

All the chemicals and RNA sequence were purchased from Sigma-Aldrich. All DNA sequences were purchased from Sangon (Shanghai, China). The synthetic route of N-methyl-N-(1,10-phenanthrolin-2-yl)-1,10-phenanthrolin-2-amine (**L1**) and N-(1,10-phenanthrolin-2-yl)-N-(2-(piperidin-1-yl)ethyl)-1,10-phenanthrolin-2-amine (**L2**) were described in supporting information. Milli-Q water was used in all physical measurement experiments. ^{195}Pt NMR spectra were recorded on a Bruker AVIII 400MHz NMR spectrometer. Chemical shift was referenced externally to K_2PtCl_4 in D_2O (δ -1628 ppm) for ^{195}Pt NMR spectra.

Synthesis of [Pt(bpa)]Cl_2 complexes

[Pt(L1)]Cl_2 (**1**). $Pt(dmso)_2Cl_2$ (11.0 mg) and **L1** (10 mg) were brought to reflux

in a mixture of methanol and water with the ratio of 1:1. After 5 hours, the mixture was cool to room temperature and yielded orange precipitates. The crudes were collected by filtration and were washed with methanol for three times to provide the product in 78% yield. ^{1}H NMR (300 MHz, DMSO-d_6) δ 9.98 (d, *J* = 4.5 Hz, H2,2', 2H), 9.35-9.25 (m, H4,4',7,7', 4H), 8.69 (d, *J* = 9.3 Hz, H8,8', 2H), 8.53-8.33 (m, H3,3',5,5',6,6', 6H), 4.53 (s, 3H). ^{195}Pt NMR (86 MHz, DMSO-d_6): δ -2272. ESI-MS calcd for $[M - Cl]^+$ 617.08, $[M - 2Cl]^{2+}$ 291.06. Found $[M - Cl]^+$ 616.96, $[M - 2Cl]^{2+}$ 290.96.

$[Pt(L2)]Cl_2$ (**2**). $Pt(dmso)_2Cl_2$ (11.0 mg) and **L2** (12.5 mg) were reflux in methanol. After 5 hours, the mixture was cool to room temperature and yielded yellow precipitates. The crudes were collected by filtration and were washed with methanol for three times to provide the product in 85% yield. ^{1}H NMR (500 MHz, DMSO-d_6) δ 10.05 (d, *J* = 4.7 Hz, H2,2', 2H), 9.38 (d, *J* = 9.2 Hz, H7,7', 2H), 9.33 (d, *J* = 8.2 Hz, H4,4', 2H), 8.90 (d, *J* = 9.2 Hz, H8,8', 2H), 8.58 (d, *J* = 8.6 Hz, H6,6', 2H), 8.52-8.45 (m, *J* = 7.6 Hz, H3,3',5,5', 4H), 5.49 (t, *J* = 7.3 Hz, H1,1', 2H), 3.86 (t, *J* = 7.3 Hz, H9,9', 2H), 3.66 (d, *J* = 11.3 Hz, H10,10', 2H), 3.15 (s, H10",10"', 2H), 1.90 (m, H11",11"',12,12' 4H), 1.80 (d, *J* = 11.7 Hz, H11, 1H), 1.52-1.37 (m, H11', 1H). ESI-MS calcd for $[M - Cl]^+$ 714.17, $[M - 2Cl]^{2+}$ 339.60. Found $[M - Cl]^+$ 715.04, $[M - 2Cl]^{2+}$ 339.19.

Thermal melting assay

Thermal melting of G-quadruplexes and double stranded DNA were obtained by CD melting. 100 μL of *c-myc* or HT21 (3 μM in 10 mM lithium cacodylate buffer,

pH = 7.4, without KCl), 100 μL of telomeric RNA (6 μM in 10 mM potassium phosphate buffer, pH = 7.0, 15 mM KCl) and 100 μL of ds26 (5 μM in 5 mM potassium phosphate buffer, pH = 7.4) were annealed by heating at 95 °C for 5 min and gradually cooling to room temperature over couple hours. Pt complexes were added to DNA solution to yield a final concentration of 3 μM or 5 μM (only for ds26). Thermal melting was monitored at 260 nm for *c-myc*, 295 nm for HT21, 263 nm for telomeric RNA and 250 nm for ds26, at the heating rate of 0.5 °C/min from 20 °C to 95 °C. Melting temperatures were analyzed by Origin 8.0 (OriginLab Corp.). Standard deviation over three repeat experiments were used as error bars.

UV-vis absorption titration

For UV titration experiment, 100 μL of Pt complex solution (20 μM in 100 mM KCl, 10 mM Tris HCl, pH 7.4) was titrated with 1 μL of DNA stock (100 μM in 100 mM KCl, 10 mM Tris HCl, pH 7.4) at 25 °C. Binding association constant K (M^{-1}) was calculated with the literature method [44]. The results were got from average of three replicates.

CD spectrum and titration

CD spectra were recorded on a Jasco J-1500 spectropolarimeter using a 1 cm path length cuvette. DNA stock solutions were diluted to 3 μM with 10 mM lithium cacodylate buffer (pH 7.4) with 1 mM KCl for *c-myc* and 10 mM KCl for HT21. 12-nt RNA stock solution was diluted to 6 μM with 10 mM potassium phosphate buffer (pH = 7.0) with 15 mM KCl, respectively. CD spectra were recorded from 220-320

nm at a scan rate of 200 nm/min after each titration of complex to DNA solutions. All CD spectra were baseline-corrected and each curve represented of five averaged scans taken at 25 °C. Final analysis of the data was carried out using Origin 8.0 (OriginLab Corp.).

Molecular docking of Pt complexes to GQ topological structures

1 and **2** were first drawn by Gaussian view followed by an optimization step (B3LYP/6-31g* for C, H, N; SDD for Pt) using Gaussian 09 to optimize the coordination structures of two Pt complexes [45]. In docking simulation, GOLD Suite v5.4 (CCDC Software Limited) is used to dock the optimized structures of two complexes, **1** and **2**, into the basket (PDB ID: 2mcc) and hybrid G-quadruplex structures (PDB ID: 2mb3), respectively [46]. Pt cation was set as a dummy atom for docking simulation. The scoring function was calculated by CHEMPLP. In each simulation, all the torsional angles within 15 Å to the binding site, i.e. the center of the external G-quartet layer, was free to rotate. Subsequently genetic algorithm was employed to find the maximum fitness value among all possible configurations and translational positions of complexes around the binding center on G-quadruplexes. For each simulation, the docking solution with largest fitness value was chosen. The docked structures of platinum complexes on GQs were visualized and the H-bond lengths were measured in VMD (NIH Center for Macromolecular Modeling and Bioinformatics, at the Beckman Institute, University of Illinois at Urbana-Champaign) [47].

Cell cytotoxicity

HeLa (human cervical epithelioid carcinoma), A549 (Human lung carcinoma) and MCF-7 (human breast adenocarcinoma) cancer cell lines were seeded in a 96-well culture plate (5000 cells per well), and incubated in DMEM medium supplemented with10% FBS, 1% L-glutamine and 1 % P/S at 37 °C with 5% CO_2 in a humidified atmosphere for 24 hours. The tested compounds were dissolved in bio-grade DMSO, diluted with DMEM medium to the required concentrations (contains <1% v/v DMSO) and added to the wells respectively. The plates were incubated at 37 °C in a 5% CO_2 incubator for 48 h continuously. After incubation, the medium was removed and 200 μL fresh medium contains MTT (20 μL, 5 mg/mL) was added to each well and the plate was incubated at 37 °C in 5% CO_2 for another 4 hours. Then the medium was removed and 150 μL DMSO was added into each well. After the plates were shaken for 10 mins, the optical density of each well was measured on a plate spectrophotometer at a wavelength of 570 nm with background subtraction at 650nm.

Results and discussion

Synthesis of $[Pt(bpa)]^{2+}$ complexes with planar structure

The two phenanthrolines in $[Pt(phen)_2]^{2+}$ provided a near square shape of aromatic area with similar size to that of a G-tetrad [39]. Previous molecular docking of $[Pt(dip)_2]^{2+}$, a $[Pt(phen)_2]^{2+}$ derivative with four corner phenyl groups, showed the two phen ligands underwent a conformation alteration to enter a flatter coordination plane upon stacking with *c-myc* GQ [48]. This phenomenon suggested a planar

geometry of Pt complexes would be essential for the high stabilization effect on G-quadruplex. The X-ray crystal structure of acidified bpa ligand was previously reported to be a near planar structure, since the aza-bridge can facilitate the two phenanthrolines to form an intramolecular H-bond network and to overcome the electron repulsion among the C2 hydrogens of the two phen rings (scheme 1) [49]. Herein, $[Pt(bpa)]^{2+}$ was expected to have a rigid planar geometry that was similar to the bound $[Pt(phen)_2]^{2+}$ on GQ. Meanwhile, the aza-bridge offered an opportunity to extend the aromatic ring with alkyl tail via facile synthetic routes. Thus, extra interaction modes with loops region would be achieved by varying the lengths and charges on alkyl tails.

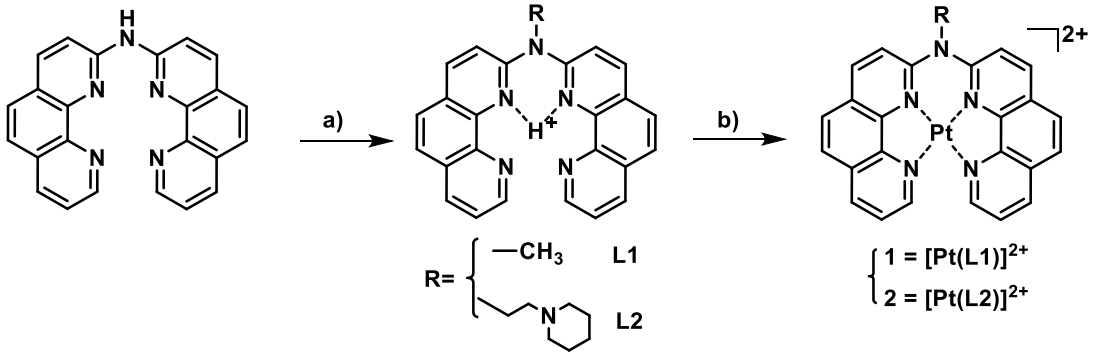

a) 1. KOH, DMSO, r.t., 30 min; 2. **1**: CH_3I, r.t., 48 h **2**:1-(2-chloroethyl)piperidine hydrochloride, 110 ^oC, 8 h; 3. acidify **1** and **2** with TFA; b) $Pt(dmso)_2Cl_2$, $MeOH/H_2O$, reflux 5 h.

Scheme 1. Synthesis of the Platinum complexes

For the synthesis of two Pt complexes, the bpa ligand was firstly synthesized as previously report [49,50]. After basified the bpa ligand, alkylation of the amino group as aza-bridge was carried out by refluxing bpa in dimethyl sulfoxide in the presence of KOH and alkylation agents (iodomethane or 1-(2-chloroethyl)piperidine). The alkylated bpa ligands were then protonated with trifluoroacetic acid so that two phenanthrolinyl moieties were stabilized into a planar structure via hydrogen bonds,

which make it ready for chelation of Pt(II) (Scheme 1). The complex structures were characterized by ^{1}H and ^{195}Pt NMR and ESI-MS (Figure S1-S4).

High efficiency of Pt complexes on stabilizing both DNA and RNA GQs

The stabilizing effects of Pt complexes on GQs and duplex DNA were first explored by thermal denaturaion of DNA. The sequences of DNA structures were listed in Table S1. Upon addition of one equivalent of **1** or **2**, significant enhancement in thermal melting temperatures of G-quadruplexes (ΔT_m) were observed for two DNA G-quadruplexes (Fig. S5). ΔT_m of telomeric DNA GQs achieved 40 °C, while decent T_m increment up to 16 °C were readily observed for *c-myc* GQ (Table 1). The discrepancy in T_m increments was presumably due to the distinct topology of telomere G-quadruplex. However, for the duplex DNA, only 4.5 and 2.0 °C incensement in melting temperatures was observed in the presence of **1** or **2,** respectively. Such insignificant ΔT_m suggested that the stabilizing abilities of Pt complexes on duplex DNA were much weaker than that on GQs. Binding affinities of this two Pt complexes to all the DNA structures was abstracted from UV-vis titration (Table S2). Although the differences in binding affinities for two Pt complexes towards GQs and duplex DNA were not as high as that in ΔT_m, K_b values still reached nearly 4 ~ 5 times higher on GQs than that on ds26.

Table 1. The increments in melting temperatures (ΔT_m)[a] of DNA by 1 and 2.

DNA	ΔT_m (°C)	
	1	2
HT21	40 (4)	38 (4)

c-myc	16 (3)	16 (4)
TERRA	15 (2)	16 (3)
ds26	4.5 (0.8)	2.0 (0.6)

a. $\Delta T_m = T_m$(Pt-DNA) - T_m (DNA), where T_m(Pt-DNA) and T_m (DNA) are CD melting temperatures of DNA structures in the presence and absence of platinum complexes, **1** or **2**, respectively.

As mentioned above, telomere sequence is transcribed into telomeric repeat-containing RNA, which was found in living cells and regarded as a promising cancer therapeutic target as well [23-25]. So far, some metal complexes have shown excellent binding affinity and stabilization on DNA G-quadruplexes, but none of them has been demonstrated as RNA G-quadruplex stabilizer. Inspired by the such high ΔT_m values on DNA G-quadruplex, the interactions of these two platinum complexes on RNG G-quadruplex were further explored. 12-nt human telomeric RNA sequence (*TERRA*) as the transcript of telomeric DNA, r(UAGGGUUAGGGU) was used in this study due to the known dimeric parallel G-quadruplexes structure characterized by NMR experiment [51]. Similar as DNA GQs, K^+ could stabilize the bimolecular *TERRA* RNA GQ by coordinating to guanines from two RNA strands. The thermal stability of *TERRA* GQ in K^+ buffer was characterized by CD melting experiments. Addition of one equivalent of **1** or **2** shifted the melting curve of *TERRA* GQ more than 15 °C towards high temperature. As expected, the bpa chelated Pt complexes showed the ability to not only stabilize DNA G-quadruplexes, but also the telomeric RNA GQ. The stabilizing ability of both Pt complexes on RNA GQ were as good as the small molecular stabilizer reported up to now, if not better, such as BRACO-19 (in the presence of 2.5 equivalents, ΔT_m for *TERRA* RNA GQ was only

up to 11.3 °C [52]). Since the two Pt complexes showed negligible difference in ΔT_m for RNA GQ, the flat aromatic core of two $[Pt(bpa)]^{2+}$ complexes had the suitable size and shape to offer dominant π-stacking effects to stabilize RNA g-tetrads in *TERRA* GQ.

Stabilizing preferences of Pt complexes toward antiparallel G-quadruplex topology

Besides the selectively stabilization effect on GQs over duplex DNA, this two Pt complexes may further distinguish and alter the folding topology of G-quadruplexes. As shown in Table 1, ΔT_m of telomeric DNA G-quadruplexes (about 40 °C) were nearly 25 °C higher than that of *c-myc* GQ (16 °C) and *TERRA* RNA GQ (15~16 °C). The thermal stability of the antiparallel HT21 GQs were elevated more significantly than that of parallel DNA and RNA GQs.

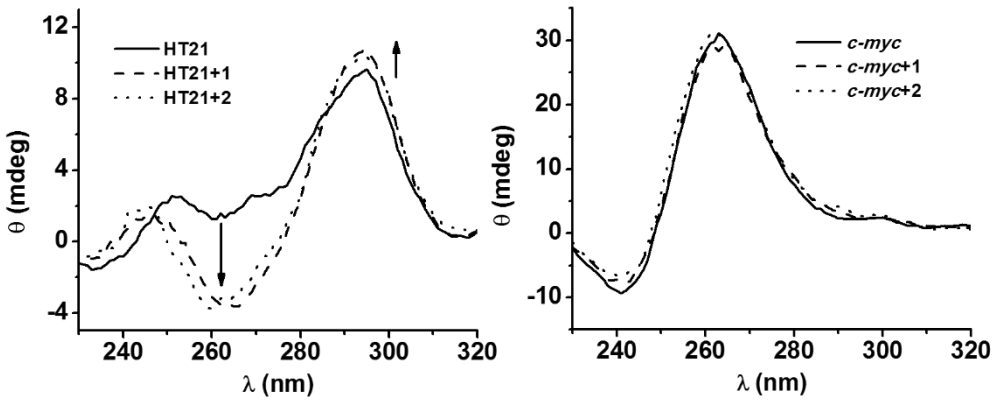

Fig. 1. CD spectra of G-quadruplexes in the presence of **1** and **2.** *Left*: **HT21.** *Right*: ***c-myc*.**

The preference of **1** and **2** to stabilize antiparallel GQs could be further evident by CD spectra (Fig. 1). In the presence of potassium ion, addition of **1** or **2** will promote a new peak at 260 nm with negative ellipticity, accompanied with the exit of the positive peak shoulder around 272 nm. Meanwhile, the major positive band at 295 nm was mildly enhanced. The spectra variation was consistent with the transition

of GQ topology from 3+1 hybrid to basket type antiparallel GQ, which indicated that **1** and **2** can efficiently and specifically induce and stabilize the basket-type GQ, even though hybrid GQ is the dominant topology in potassium buffer [9,53,54]. On the contrary, the folding structure of both *c-myc* GQ and dimeric *TERRA* RNA GQ have been determined as a parallel topology with propeller-type structure. Little variation in CD spectra of both parallel GQ upon the addition of **1** or **2** was observed, regardless the distinct conformation of backbone pentose (Fig.1 and S6). The discrepancy that both Pt complexes showed on the folding topology and thermal stability of parallel and anti-parallel GQs, suggested that the planar coordination geometry in **1** and **2** likely possessed a strong inclination to antiparallel GQ, especially basket-type folding topology, and achieve remarkably high stabilizing effects.

Molecular docking of Pt complexes on different GQ structures

Table 2. Best fitting values of molecular docking of **1** and **2** on various GQ topological structures.

GQ topology (PDB code)	basket type (2MCC)	3+1 hybrid (2MB3)	parallel *c-myc* (1XAV)
1	89.6	82.4	57.4
2	103.7	95.3	67.0

Since topological folding of GQ cannot be exclusively demonstrated by CD spectra [55], molecular docking of Pt complexes on three different GQ structures, basket (PDB 2MCC), 3+1 hybrid (2MB3) and parallel GQ (1XAV) were utilized to provide further information for topological selectivity of Pt complexes favoring

antiparallel GQ over parallel structure, especially to basket G-quadruplex. Pt complexes showed remarkably higher fitting values on basket and hybrid 3+1 G-quadruplexes topologies (>82) than the parallel structure (<67), which is consistent with the observations on the thermal stability and CD spectra of both RNA and DNA GQs. Both **1** and **2** achieved higher fitting values on basket GQ than 3+1 hybrid GQ (Table 2) indicating the inclination to basket folding topology. In the best docking structure, Pt complexes stacked on top of the external G-quartet in the dual lateral loop side (Fig. 2a, S7a). From the top view (Fig. 2b, S7b), the bpa ligand showed an appropriate size to overlap exactly right on top of the aromatic area of G-quartet. On the contrary, both **1** and **2** would disturb the flatness of G-quartet upon stacking on 3+1 hybrid GQ (Fig. 2c, S7c). The discrepancy in the fitting values and docking structures of Pt complexes on different GQ structures confirmed the better accommodation of both Pt complexes to basket type GQ with a higher stability, which also supported the conversion of CD spectra from 3+1 hybrid GQ to basket GQ upon binding to Pt complexes.

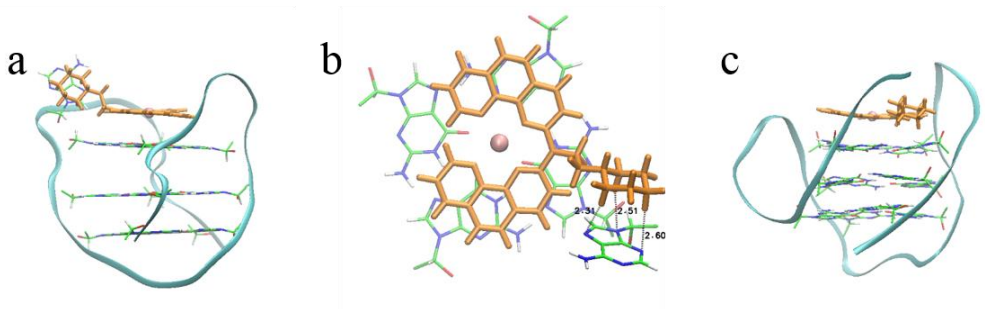

Fig. 2. Molecular docking of **2** on basket (PDB: 2mcc, *a*: side view; *b*: top view,) and 3+1 hybrid GQ (PDB: 2mb3, *c*: side view). Backbone and G-quartets in both quadruplexes were represented as cyan ribbon and in stick mode, respectively. **2** and Pt cation were shown in orange stick and pink ball, respectively.

Effects of the alkyl side chains on distinguishing DNA structures

1 and **2** showed 4.5 and 2.0 °C of ΔT_m on duplex DNA, respectively. Stabilizing ability of **2** on duplex was decreased comparing with **1**, which ΔT_m was similar as that of $[Pt(phen)_2]^{2+}$ [47]. This suggested that longer alkyl chain with a bulky piperidinium terminal in **2** prevent the aromatic ligand in complexes from binding or intercalating into duplex DNA. Remarkably, compared with $[Pt(phen)_2]^{2+}$, 5 folds higher ΔT_m value on HT21 GQ was achieved by $[Pt(bpa)]^{2+}$ complexes, while interactions with duplex DNA were comprised. Hence, the pre-planar conformation in $[Pt(bpa)]^{2+}$ complexes obviously enhanced the binding specificity to G-quadruplexes, while a flexible positive alkyl tail from aza-bridge improved the selectivity over duplex DNA.

Although the melting temperature incensements of GQs upon addition of **1** and **2** were nearly the same, the fitting values of the two complexes on the same GQ structure indicated a difference. Fitting value of **2** to the basket topology was much higher than those of **1**, which was presumably due to the extra hydrogen bonds and/or electrostatic/hydrophobic effects between the loop backbone/nucleobases of GQ and the aza-alkyl tail in **2** (Fig. 2b). Docking **2** on the basket GQ resulted in the conformation that the alkyl tail resided in the groove next to 3'-terminal. The piperidinium ring was placed parallel to an adenine base in the lateral loop in which several methylene hydrogens were within the distance of hydrogen bonds with purine nitrogens (Fig. 2b). Whereas in the case of 3+1 hybrid topology, not only these interactions were absence, but accommodation of the alkyl tail into the narrow groove

between 3' and 5' terminals altered both the orientation of Pt complex and the flatness of G-tetrads (Fig. 2c), which would significantly comprise the stability of hybrid GQ and GQ-**1**/GQ-**2** as one biological motif.

In our previous work, the aromatic anchors from two phen ligands in $[Pt(Dip)_2]^{2+}$ bestow a high binding preference on parallel G-quadruplex, while the current study showed that $[Pt(bpa)]^{2+}$ complexes with pre-planar structure exhibited much higher stabilization effects on antiparallel topology. The piperidinium tail showed extra interaction modes with loops region, which assisted the conformation conversion of HT GQ from 3+1 hybrid to basket structure. Hence, by properly tuning the flatness and the peripheral moieties of bis-phen coordination core, Pt complexes were readily to specifically target distinct GQ topological structures, regardless of the backbone composition.

Potential cytotoxicity towards cancer cells

Table 3. Cytotoxicity (IC_{50}) of **1** and **2** compared with TMPyP4 and cisplatin towards various cancerous cell lines.[a]

	IC_{50} (μM)			
	TMPyP4	**Cisplatin**	**1**	**2**
Hela	19 (3)	13 (1)	2.2 (0.1)	3.6 (0.1)
A549	43 (1) [56]	36 [57]	0.351 (0.002)	1.46 (0.01)
MCF-7	90 (3)	15 [57]	1.46 (0.04)	3.98 (0.04)

[a] Standard deviation were listed in parentheses.

The aforementioned results demonstrated the two Pt complexes could efficiently stabilize different DNA GQs, as well as telomeric RNA G-quadruplex. These findings encourage us to further investigate the biological activities of the complexes.

In vitro cytotoxicity of **1** and **2** against HeLa (human cervical epithelioid carcinoma), A549 (Human lung carcinoma) and MCF-7 (human breast adenocarcinoma) cancer cell lines were evaluated by MTT assay. IC_{50} values of **1** and **2** against all the cell lines were from 0.4 to 4 μM, as shown in Table 3. While the cell viability of A549, the most sensitive cancer cell line towards Pt complexes, was still more than 50% when 100 μM of the ligands (L1 and L2) or the precursor ($Pt(dmso)_2Cl_2$) were treated alone (Figure S8). This confirmed that the potent cell cytotoxicity were caused by $[Pt(bpa)]^{2+}$ as a complex, but neither ligand or metal core as individual component. The potency of Pt complexes here was nearly 9 and 6 times more potent than the well-known GQ stabilizer, TMPyP4 and chemotherapy drug, cis-platin, respectively.

Conclusion

In this study, two Pt complexes coordinated with aza-bridged bis-phenanthroline ligands were designed and synthesized. The aza-bridge enabled the complexes to obtain a flat aromatic structure even prior to the binding of G-quadruplex and achieve remarkably high stabilizing effects on both human telomeric DNA and RNA G-quaruplexes. The alkyl chain extended from aromatic core further decreased the binding and stabilization of the complexes on duplex DNA and hence enhanced the binding specificity towards G-quadruplex. Moreover, both complexes showed topological preferences towards basket-type of antiparallel G-quadruplex evidenced by higher thermal stability and alteration of hybrid to basket GQ folding conformation even in the potassium buffer. The stabilizing effects on human telomeric GQ rendered potent cytotoxicity of the complexes towards a wide range of

the cancer cell lines that showed high potentials of the complexes as drug candidates for anticancer therapy.

Acknowledgement

Authors would like to thank the Nanyang Assistant Professor Fellowship (M4080531) and Singapore Ministry of Education AcRF Tier 2 Research Grant (M4020163) for the research fund support.

References

[1] W. Guschlbauer, J. F. Chantot, D. Thiele, J. Biomol. Struct. Dyn. 8 (1990) 491-511.
[2] M. Gellert, M. N. Lipsett, D. R. Davies, Proc. Natl. Acad. Sci. U. S. A. 48 (1962) 2013-2018.
[3] S. B. Zimmerman, G. H. Cohen, D. R. Davies, J. Mol. Boil. 92 (1975) 181-192.
[4] J. R. Williamson, Annu. Rev. Biophys. Biomol. Struct. 23 (1994) 703-730.
[5] J. T. Davis, Angew. Chem. Int. Ed. 43 (2004) 668-698.
[6] S. Neidle, S. Balasubramanian, The Role of Cations in Determining Quadruplex Structure and Stability. In *Quadruplex Nucleic Acids,* The Royal Society of Chemistry (2006) 100-130.
[7] D. Sen, W. Gilbert, Nature 344 (1990) 410-414.
[8] Y. Xu, Y. Noguchi, H. Sugiyama, Bioorg. Med. Chem. 14 (2006) 5584-5591.
[9] A. Ambrus, D. Chen, J. Dai, T. Bialis, R. A. Jones, D. Yang, Nucleic Acids Res. 34 (2006) 2723-2735.
[10] G. N. Parkinson, M. P. Lee, S. Neidle, Nature 417 (2002) 876-880.
[11] K. W. Lim, L. Lacroix, D. J. E. Yue, J. K. C. Lim, J. M.W. Lim, A. T. Phan, J. Am. Chem. Soc. 132 (2010) 12331-12342.
[12] K. N. Luu, A.T. Phan, V. Kuryavyi, L. Lacroix, D. J. Patel, J. Am. Chem. Soc. 128 (2006) 9963-9970.
[13] P. Šket, M. Črnugelj, J. Plavec, Nucleic Acids Res. 33 (2005) 3691-3697.
[14] A.T. Phan, Febs J. 277 (2010) 1107-1117.
[15] S. Burge, G. N. Parkinson, P. Hazel, A. K. Todd, S. Neidle, Nucleic Acids Res. 34 (2006) 5402-5415.
[16] E. Largy, A. Marchand, S. Amrane, V. Gabelica, J. L. Mergny, J. Am. Chem. Soc. 138 (2016) 2780-2792.
[17] K.W. Lim, V. C. M. Ng, N. Martín-Pintado, B. Heddi, A. T. Phan, Nucleic Acids Res. 41 (2013) 10556-10562.
[18] R. K. Moyzis, J. M. Buckingham, L. S. Cram, M. Dani, L. L. Deaven, M. D. Jones, J. Meyne, R. L. Ratliff, J. R. Wu, Proc. Natl. Acad. Sci. U. S. A. 85 (1988) 6622-6626.

[19] J. Meyne, R. L. Ratliff, R. K. MoYzIs, Proc. Natl. Acad. Sci. U. S. A. 86 (1989) 7049-7053.
[20] W. E. Wright, V. M. Tesmer, K. E. Huffman, S. D. Levene, J. W. Shay, Genes Dev. 11 (1997) 2801-2809.
[21] C. Punchihewa, D. Yang, Telomeres and Telomerase in Cancer, Springer 2009, pp. 251-280.
[22] S. Neidle, G. Parkinson, Nat. Rev. Drug Discov. 1 (2002) 383-393.
[23] B. Luke, J. Lingner, EMBO J. 28 (2009) 2503-2510.
[24] C. Caslini, J. A. Connelly, A. Serna, D. Broccoli, J. L. Hess, Mol. Cell. Boil. 29 (2009) 4519-4526.
[25] S. Redon, P. Reichenbach, J. Lingner, Nucleic Acids Res. 38 (2010) 5797–5806.
[26] D. Hanahan, R. A. Weinberg, Cell 100 (2000) 57-70.
[27] K. Shin-ya, K. Wierzba, K. i. Matsuo, T. Ohtani, Y. Yamada, K. Furihata, Y. Hayakawa, H. Seto, J. Am. Chem. Soc. 123 (2001) 1262-1263.
[28] C. M. Barbieri, A. R. Srinivasan, S. G. Rzuczek, J. E. Rice, E. J. LaVoie, D. S. Pilch, Nucleic Acids Res. 35 (2007) 3272-3286.
[29] M. Y. Kim, H. Vankayalapati, K. Shin-ya, K. Wierzba, L.H. Hurley, J. Am. Chem. Soc. 124 (2002) 2098-2099.
[30] F. X. Han, R. T. Wheelhouse, L. H. Hurley, J. Am. Chem. Soc. 121 (1999) 3561-3570.
[31] R. J. Harrison, J. Cuesta, G. Chessari, M. A. Read, S. K. Basra, A. P. Reszka, J. Morrell, S. M. Gowan, C. M. Incles, F. A. Tanious, J. Med. Chem. 46 (2003) 4463-4476.
[32] W. J. Chung, B. Heddi, F. Hamon, M. P. Teulade-Fichou, Angew. Chem. Int. Ed. 53 (2014) 999-1002.
[33] I. M. Dixon, F. Lopez, A. M. Tejera, J. P. Estève, M. A. Blasco, G. Pratviel, B. Meunier, J. Am. Chem. Soc. 129 (2007) 1502-1503.
[34] D. Monchaud, P. Yang, L. Lacroix, M. P. Teulade-Fichou, J.L. Mergny, Angew. Chem. 120 (2008) 4936-4939.
[35] J. E. Reed, A. A. Arnal, S. Neidle, R. Vilar, J. Am. Chem. Soc. 128 (2006) 5992-5993.
[36] R. Kieltyka, P. Englebienne, J. Fakhoury, C. Autexier, N. Moitessier, H. F. Sleiman, J. Am. Chem. Soc. 130 (2008) 10040-10041.
[37] V. S. Stafford, K. Suntharalingam, A. Shivalingam, A. J. White, D. J. Mann, R. Vilar, Dalton Trans. 44 (2015) 3686-3700.
[38] A. J. Gaier, D. R. McMillin, Inorg. Chem. 54 (2015) 4504-4511.
[39] J. T. Wang, X. H. Zheng, Q. Xia, Z. W. Mao, L. N. Ji, K. Wang, Dalton Trans. 39 (2010) 7214-7216.
[40] P. Wang, C. H. Leung, D. L. Ma, S. C. Yan, C. M. Che, Chem. Eur. J. 16 (2010) 6900-6911.
[41] K. Suntharalingam, A. J. White, R. Vilar, Inorg. Chem. 48 (2009) 9427-9435.
[42] R. Kieltyka, J. Fakhoury, N. Moitessier, H.F. Sleiman, Chem. Eur. J. 14 (2008) 1145-1154.
[43] D. L. Ma, C. M. Che, S. C. Yan, J. Am. Chem. Soc. 131 (2008) 1835-1846.

[44] R. Kieltyka, P. Englebienne, N. Moitessier, H. Sleiman, G-Quadruplex DNA: Methods and Protocols, (2010) 223-255.
[45] M. J. Frisch, et. al., Gaussian 09, Gaussian, Inc., Wallingford, CT, USA, 2009.
[46] G. Jones, P. Willett, R. C. Glen, J. Mol. Boil. 245 (1995) 43-53.
[47] W. Humphrey, A. Dalke, K. Schulten, J. Mol. Graph. 14 (1996) 33-38.
[48] J. Wang, K. Lu, S. Xuan, Z. Toh, D. Zhang, F. Shao, Chem. Commun. 49 (2013) 4758-4760.
[49] H. C. Kao, C. J. Hsu, C. W. Hsu, C. H. Lin, W. J. Wang, Tetrahedron Lett. 51 (2010) 3743-3747.
[50] J. Concepción, O. Just, A.M. Leiva, B. Loeb, W.S. Rees, Inorg. Chem. 41 (2002) 5937-5939.
[51] H. Martadinata, A.T. Phan, J. Am. Chem. Soc. 131 (2009) 2570-2578.
[52] G. Collie, A. P. Reszka, S. M. Haider, V. Gabelica, G. N. Parkinson, S. Neidle, Chem. Commun. (2009) 7482-7484.
[53] Z. Zhang, J. Dai, E. Veliath, R.A. Jones, D. Yang, Nucleic Acids Res. 38 (2010) 1009-1021.
[54] L. He, X. Chen, Z. Meng, J. Wang, K. Tian, T. Li, F. Shao, Chem. Commun. 52 (2016) 8095-8098.
[55] J. Joaquim and G. Raimundo, Curr. Pharm. Design 18, (2012) 1900-1916.
[56] T. Taka, K. Joonlasak, L. Huang, T. R. Lee, S. W. T. Chang, W. Bioorg. Med. Chem. Lett. 22 (2012) 518-522.
[57] S. Tardito, C. Isella, E. Medico, L. Marchiò, E. Bevilacqua, M. Hatzoglou, O. Bussolati, R. Franchi-Gazzola, J. Biol. Chem. 284 (2009) 24306-24319.

Supporting Materials for

Aza-bridged bisphenanthrolinyl Pt(II) complexes: efficient stabilization and topological selectivity on telomeric G-quadruplexes

Lei He[#1], Zhenyu Meng[#1], Yiqun Xie[#2], Xiang Chen[1], Tianhu Li[1], Fangwei Shao[1]*

[1]*Division of Chemistry and Biological Chemistry, School of Physical and Mathematical Sciences, Nanyang Technological University, Singapore 637371*
[2]*Department of Breast Surgery, Shanghai Huangpu Center Hospital, Shanghai, China 200002*

Synthesis of N-methyl-N-(1,10-phenanthrolin-2-yl)-1,10-phenanthrolin-2-amine (L1)

N,N-Bis-(1,10-phenanthrolin-2-yl)-amine (bpa) was prepared as previously reported.[1,2] Into DMSO (3 mL) were successively added potassium hydroxide (17 mg) and bpa (20 mg). The resulting deep-orange-colored solution was stirred at r.t. for 30 min. Iodomethane (12.4 μL) was then added and the orange solution was stirred at r.t. for 48 h, and then diluted with water (20 mL), which lead to the immediate deposition of a fine yellow precipitate and was collected by filtration. After washing with water, the yellow solid was dried to yield the compound (80% yield). ^{1}H NMR (500 MHz, DMSO) δ 9.09 (dd, *J* = 4.2, 1.5 Hz, H2,2', 2H), 8.45 (dd, *J* = 8.1, 1.5Hz, H4,4', 2H), 8.40 (d, *J* = 8.8 Hz, H7,7', 2H), 7.98 (d, *J* = 8.8 Hz, H6,6', 2H), 7.96 (d, *J* = 8.8 Hz, H5,5', 2H), 7.86 (d, *J* = 8.8 Hz, H8,8', 2H), 7.74 (dd, *J* = 8.1, 4.2 Hz, H3,3', 2H), 4.09 (s, H1,1',1", 3H). ESI-MS (M+H) = 388.41.

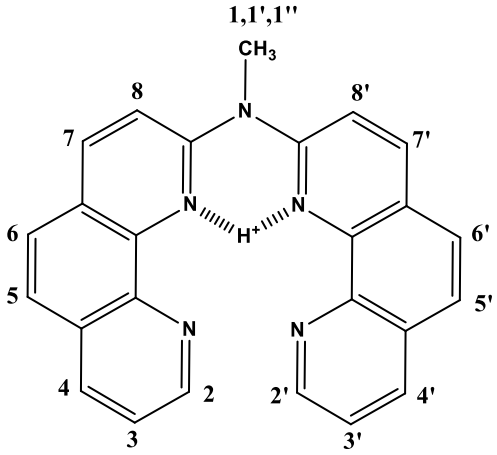

Synthesis of N-(1,10-phenanthrolin-2-yl)-N-(2-(piperidin-1-yl)ethyl)-1,10-phenanthrolin-2-amine (L2)

Into dimethyl sulfoxide were successively added potassium hydroxide (7.8 mg) and bpa (10 mg). The resulting deep-orange colored solution was stirred at room temperature

for 2 h. 1-(2-chloroethyl)piperidine hydrochloride (8.4 mg) was then added and the orange solution was stirred at 110 °C for 8 h. It was then diluted with water, which lead to the immediate deposition of a yellow precipitate and was collected by filtration. The precipitate was washed with water for several times to yield the compound (40 % yield). ^{1}H NMR (300 MHz, MeOD) δ 9.01 (dd, *J* = 4.4, 1.7 Hz, H2,2', 2H), 8.43 (dd, *J* = 8.2, 1.7 Hz, H4,4', 2H), 8.26 (d, *J* = 8.8 Hz, H7,7', 2H), 7.88 (d, *J* = 8.8 Hz, H6,6', 2H), 7.79 (d, *J* = 8.8 Hz, H5,5', 2H), 7.72 (dd, *J* = 8.2, 4.4 Hz, H3,3', 2H), 7.71 (d, *J* = 8.8 Hz, H8,8', 2H), 5.10 (t, *J* = 6.8 Hz, H1,1', 2H), 2.95 (t, *J* = 6.8 Hz, H9,9', 2H), 2.63-2.53 (m, H10,10',10",10"', 4H), 1.43-1.25 (m, H11,11',11",11"',12,12', 6H). ESI-MS (M+H) = 485.26.

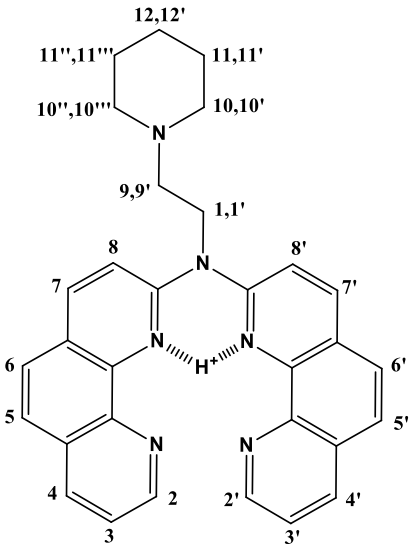

References:

[1] H. C. Kao, C. J. Hsu, C. W. Hsu, C. H. Lin, W. J. Wang, Tetrahedron Lett. 51 (2010) 3743-3747.

[2] L. He, X. Chen, Z. Meng, J. Wang, K. Tian, T. Li, F. Shao, Chem. Commun. 52 (2016) 8095-8098.

Table S1. Sequences of oligomers (primers) used in this work.

Name	Sequence
ds26	5'-CAATCGGATCGAATTCGATCCGATTG-3'
c-myc	5'-TGGGGAGGGTGGGGAGGGTGGGGAAGG-3'
HT21	5'-GGGTTAGGGTTAGGGTTAGGG-3'
TERRA	5'-uaggguuagggu-3'[a]

[a] TERRA is a 12-mer RNA strand.

Table S2. Binding constants (K_b) of DNA structures with Pt complexes **1** and **2**

DNA	K_b ($\times 10^5$ M^{-1})	
	Pt1	**Pt2**
ds26	1.8 (0.4)	2.4 (0.1)
c-myc	7.9 (0.8)	9.7 (0.4)
HT21	9.7 (0.4)	11.2 (0.2)

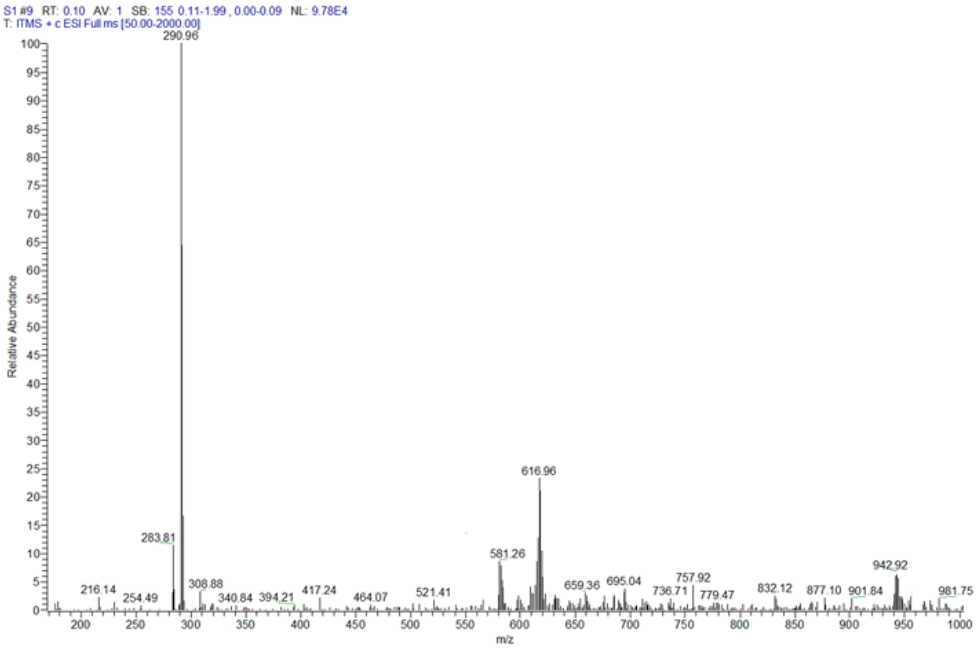

Fig. S1. Mass spectrum of **1**.

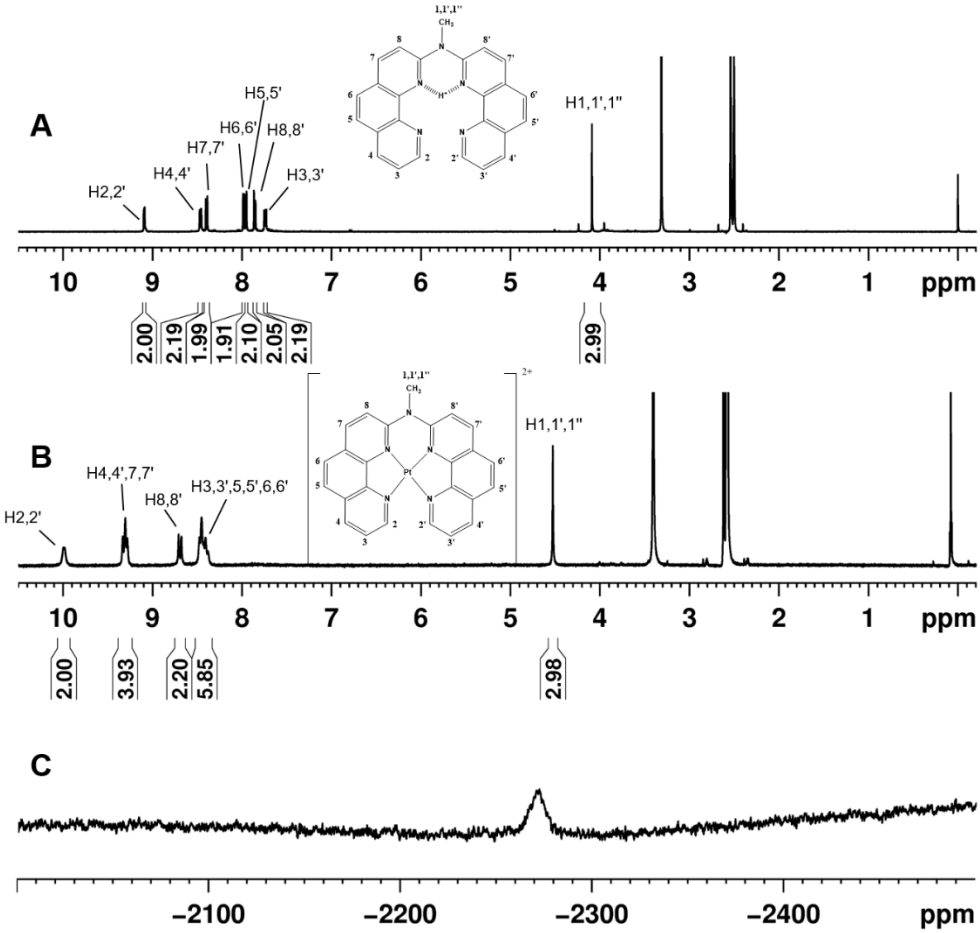

Fig. S2. ^{1}H NMR spectrum of (A) **L1** (in DMSO-d_6); (B) **1** (in DMSO-d_6) and (C) ^{195}Pt NMR of **1** (in DMSO-d_6).

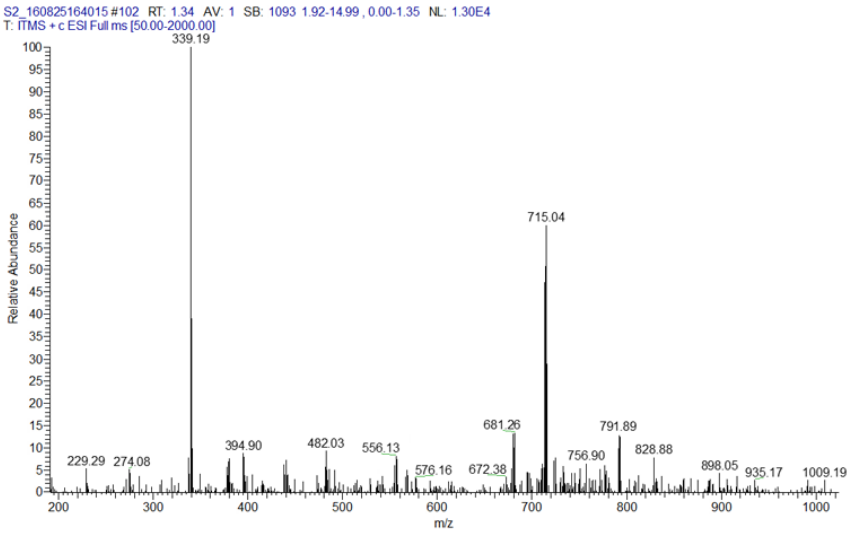

Fig. S3. Mass spectrum of **2**.

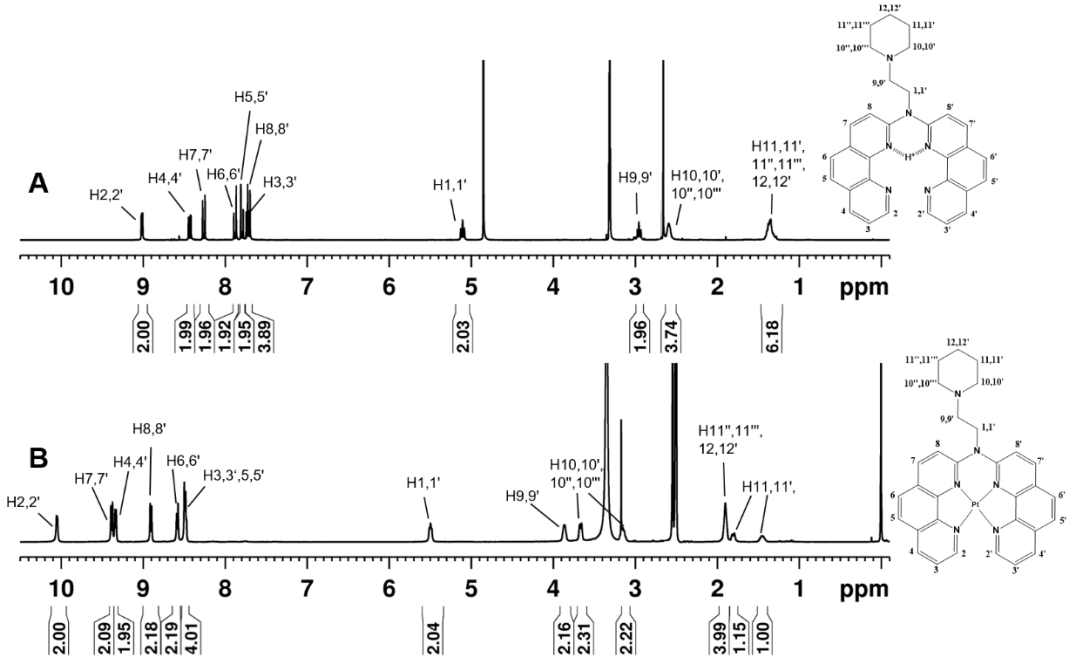

Fig. S4. ^{1}H NMR spectrum of (A) **L2** (in Methanol-d_4); (B) **2** (in DMSO-d_6).

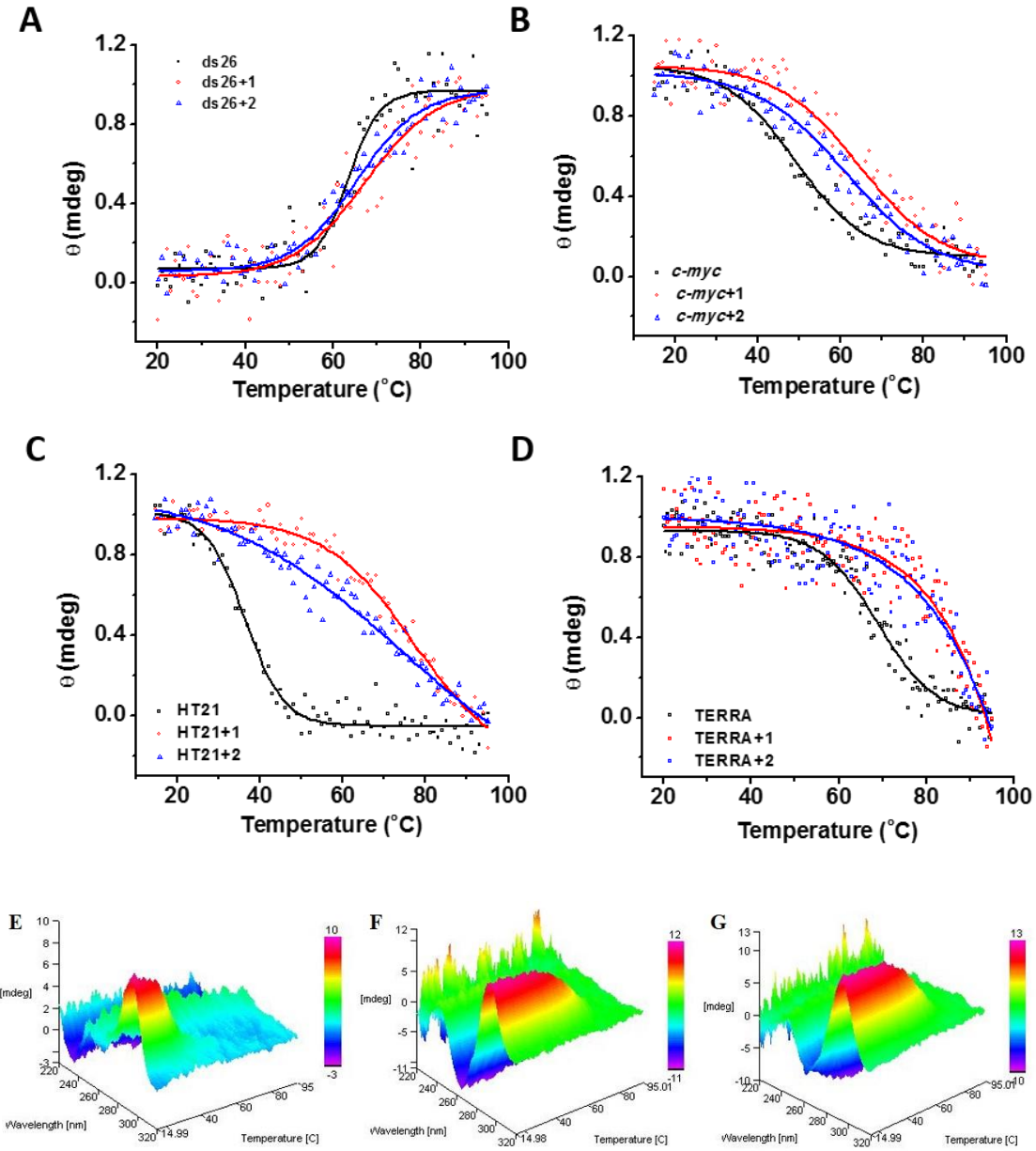

Fig. S5. (A-D) CD Melting of ds26, *c-myc*, HT21 and TERRA in the presence and absence of **1** and **2**. (E-F) The CD spectra of HT21 along with temperature elevation. (E) HT21 alone; (F) HT21 with **1**; (G) HT21 with **2**.

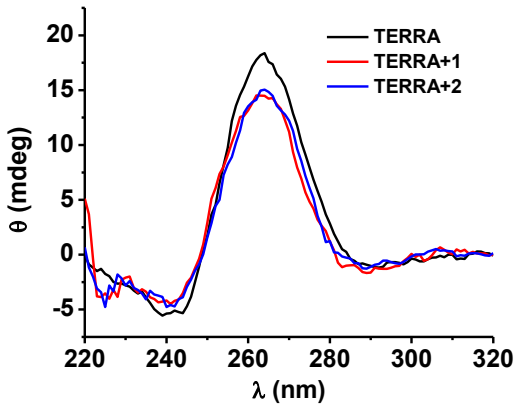

Fig. S6. CD spectra of TERRA G-quadruplex in the absence (black) and presence of **1** (red) and **2** (blue).

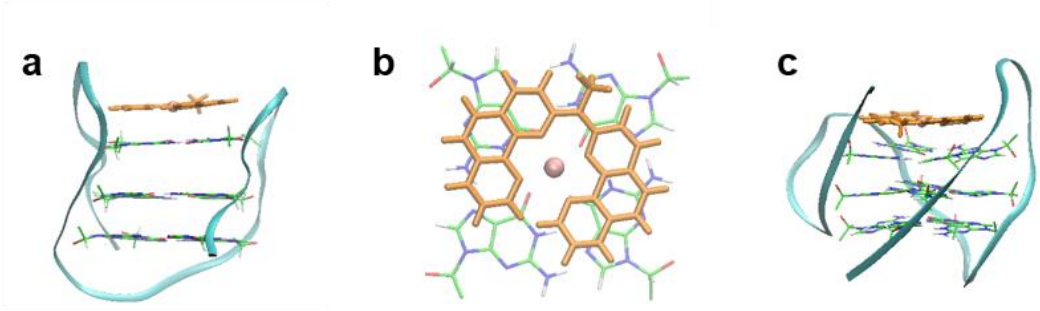

Fig. S7. Molecular docking of **1** on basket (*a*, PDB: 2mcc) and 3+1 hybrid GQ (*c*, PDB: 2mb3). *b.* Top view of aromatic overlap between **1** and G-quartet in figure *a*. Backbone and G-quartets in both quadruplexes were represented as cyan ribbon and in stick mode, respectively. **1** and Pt cation were shown in orange stick and pink ball, respectively.

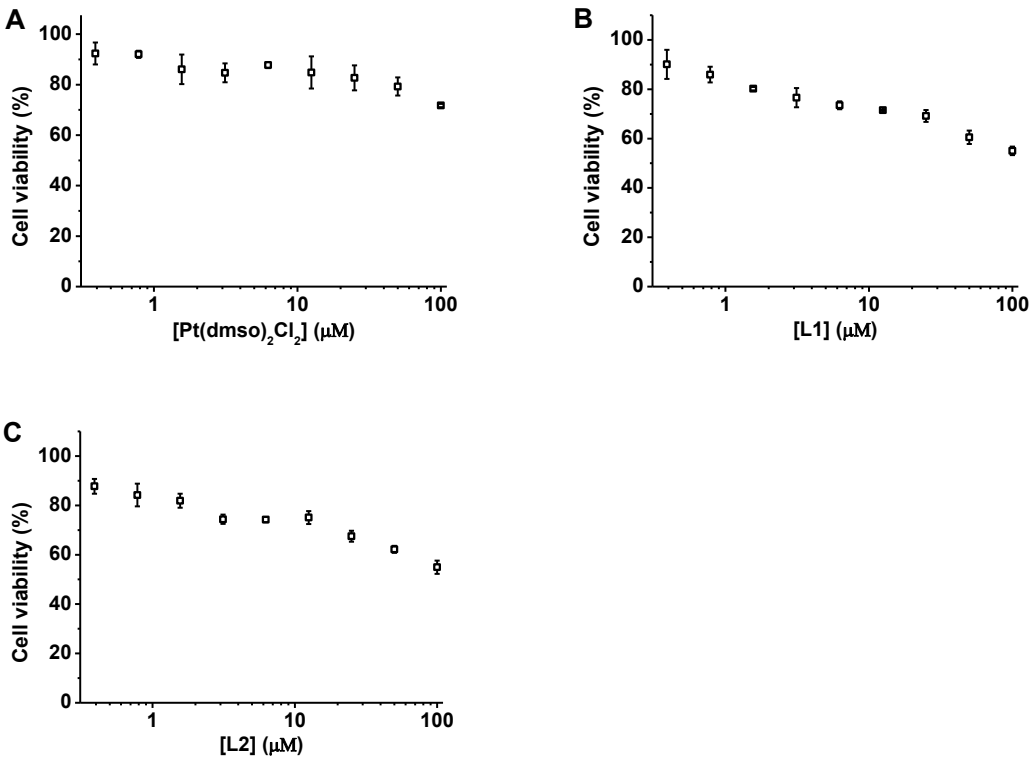

Fig. S8. Viability of the A549 cell in the presence of 0.4 ~ 100 μM (A) $Pt(dmso)_2Cl_2$; (B) L1 and (C) L2.